Title
3D-Printed Sugar-Based Stents Facilitating Vascular Anastomosis

Journal
Advanced Healthcare Materials, 7(24)

ISSN
2192-2640

Authors
Farzin, Ali
Miri, Amir K
Sharifi, Fatemeh
et al.

Publication Date
2018-12-01

DOI
10.1002/adhm.201800702

Peer reviewed

ADVANCED HEALTHCARE MATERIALS
www.advhealthmat.de

3D-Printed Sugar-Based Stents Facilitating Vascular Anastomosis

Ali Farzin, Amir K. Miri, Fatemeh Sharifi, Negar Faramarzi, Arian Jaberi, Azadeh Mostafavi, Ricky Solorzano, Yu Shrike Zhang, Nasim Annabi, Ali Khademhosseini, and Ali Tamayol**

Microvascular anastomosis is a common part of many reconstructive and transplant surgical procedures. While venous anastomosis can be achieved using microvascular anastomotic coupling devices, surgical suturing is the main method for arterial anastomosis. Suture-based microanastomosis is time-consuming and challenging. Here, dissolvable sugar-based stents are fabricated as an assistive tool for facilitating surgical anastomosis. The nonbrittle sugar-based stent holds the vessels together during the procedure and are dissolved upon the restoration of the blood flow. The incorporation of sodium citrate minimizes the chance of thrombosis. The dissolution rate and the mechanical properties of the sugar-based stent can be tailored between 4 and 8 min. To enable the fabrication of stents with desirable geometries and dimensions, 3D printing is utilized to fabricate the stents. The effectiveness of the printed sugar-based stent is assessed ex vivo. The fabrication procedure is fast and can be performed in the operating room.

1. Introduction

Vascular anastomosis is routinely performed during surgical procedures such as organ and tissue transplants as well as head, neck, and hand reconstruction.[1] For example, in 2015, more than one million reconstructive procedures were done in the US. In these surgeries, transplanted healthy tissue (free flap) is moved and implanted to the injury site. A major cause of free flap transfer failures is technical problems associated with vascular anastomoses, such as intima lacerations, distortion of the vessels, and unequal intersuture distances.[2] Failure in anastomosis results in thrombosis and, ultimately, flap failure. The traditional surgical technique for microvascular anastomosis involves stopping the blood flow using a clamp and holding the vessel sides next to each other and connecting them by using microvascular sutures (8-0 or 9-0 nylon) under a microscope.[3] Venous anastomosis can also be performed using microvascular anastomotic coupling devices.[4] The anastomotic site is rigidly stented open by the external rings, which protects against vessel collapse or spasm. The coupler creates an intima-to-intima contact without the use of sutures, which in turn reduces the chance of thrombosis.[5] Potential challenges associated with anastomotic couplers use include possible vessel twisting during coupling and potential intima trauma.[6] These couplers are also nondegradable and cannot be opened if necessary. Although effective for venous anastomoses, such couplers cannot be used for arterial anastomosis. Despite the significant advancements in the development of

Dr. A. Farzin, Dr. A. K. Miri, F. Sharifi, Dr. N. Faramarzi, Dr. Y. S. Zhang, Prof. N. Annabi, Prof. A. Khademhosseini, Prof. A. Tamayol
Division of Engineering in Medicine
Department of Medicine
Brigham and Women's Hospital
Harvard Medical School
Boston, MA 02139, USA
E-mail: khademh@ucla.edu; atamayol@unl.edu

F. Sharifi
School of Mechanical Engineering
Sharif University of Technology
Tehran 14588-89694, Iran

A. Jaberi
School of Mechanical Engineering
Shiraz University
Shiraz 71936-16548, Iran

The ORCID identification number(s) for the author(s) of this article can be found under https://doi.org/10.1002/adhm.201800702.

DOI: 10.1002/adhm.201800702

A. Mostafavi, Prof. A. Tamayol
Department of Mechanical and Materials Engineering
University of Nebraska
Lincoln, NE 68588, USA

R. Solorzano
Allevi Inc.
Philadelphia, PA 19146, USA

Prof. A. Khademhosseini
Center of Nanotechnology
Department of Physics
King Abdulaziz University
Jeddah 21569, Saudi Arabia

Prof. A. Khademhosseini
Center for Minimally Invasive Therapeutics (CMIT)
Department of Bioengineering
Department of Chemical and Biomolecular Engineering
Department of Radiology
California NanoSystems Institute (CNSI)
University of California
Los Angeles, CA 90095, USA

surgical glues, their use for vascular anastomosis is not feasible as they may leak into the blood vessels leading to blockage and thrombosis.[7] Thus, in arterial anastomosis, the only possible option is to connect the vessels through suturing, which can be time-consuming and challenging.

Suture-based anastomosis becomes more challenging when the blood vessels have different sizes, which is frequently observed in flap transplant and reconstructive surgeries.[8] In these cases, the outcome is highly skill-dependent and always carries the risk of vessel blockage or rupture. Therefore, developing an approach that facilitates suture-based anastomosis and makes the procedure less skill dependent is of great importance. One of the recent solutions that utilized a thermo-responsive poloxamer gel that could keep the vessels open during the procedure could facilitate suture-based anastomosis;[9] however, it could not eliminate the risk of vessel blockage.

Stents are widely used in medicine for keeping lumens and conduits open and reliving obstructions permanently or for a specific period of time.[10] The majority of stents are permanent and fabricated from biocompatible metals such as titanium, cobalt–chromium, and stainless steel.[11] Recently, degradable stents have been fabricated using resorbable metals such as zinc and magnesium alloys as well as hard polymers.[12] However, there have been a limited number of materials for developing temporary stents for applications where the stents are only required for short periods of time (less than an hour). Among different materials used for engineering dissolvable stents, sugar-based compounds have shown promising results.[13] However, sugar-based materials have thrombogenesis potential.[14] This will be of great concern for microsurgeries where the variation in the cross-sectional area at the sent site is significant. To address this challenge, in a study heparin was incorporated into sugar-based materials to prevent thrombosis in rabbit models.[15] However, the ability to tune the adhesion strength and dissolution rate of the stent was not addressed. In addition, using heparin at high concentrations can potentially have side effect especially in patients with low blood clotting factors.[16] Sodium citrate is a calcium chelator that is widely used in clinical practice for blood preservation. Sodium citrate toxicity range has been reported to be above 24 mg kg^{-1} day^{-1} of body weight.[17] Thus for a human with an average mass of 60 kg the toxic range is around 1440 mg. It has been shown that the citrate concentration of around 3% (w/w) is sufficient for clot prevention.[18] Thus, using sugar-based stent incorporated with sodium citrate could reduce its thrombogenicity.

Another limitation of the existing sugar-based stents is the fabrication of stents with desirable geometries and dimensions that can be used for nonequal vessel anastomosis, which is commonly seen in reconstructive surgeries. It is important to note that the size of blood vessels varies from patient to patient and thus the ability of fabricating stents with desired geometry and architecture would also significantly improve the success of such systems in microsurgeries.

The 3D printing technologies have emerged as promising tools for engineering complex yet highly defined architectures.[19] The majority of extrusion-based printers are operating on melt-extrusion process. In 3D printing with melt-extrusion technology (MET), a polymer or solid material is melted, then extruded through the nozzle, and solidified on the printing pad to form a 3D architecture.[20] The resolution of the printing is dictated by the nozzle size, the viscosity of the molten polymer, the solidification rate, and moving speed of the nozzle. Printers with MET are normally working with hard polymers and printing of soft and glassy materials is extremely challenging. Sugar materials become glassy and highly viscous once melted. The solidification process of sugar glass is also gradual, which makes their use for 3D printing challenging. There are only a few examples in the literature that have successfully 3D-printed sugar-based constructs.[21]

In this study, sugar glass is used to 3D print stents with tunable dissolution rate that prevent clot formation and can hold tissues together during the anastomosis process. The sugar composition is optimized to achieve suitable tissue adhesion, dissolution rate, printability, and clot prevention. This approach can be later on applied for printing stents with the right dimensions during the operation to improve the outcome of the process.

2. Results and Discussions

The goal of this study was to develop a dissolvable stent that could facilitate surgical anastomosis. Ideally, the stent should be nonbrittle to avoid its breakage into pieces in response to applied mechanical forces. Also, the stent should be adhesive to vessel walls to keep them in place during the surgical anastomosis. The stents should also remain stable during the surgical process, while they should dissolve rapidly following the blood flow restoration. Sugar-based structures have been previously used during vascular anastomosis. However, the utilized molding technique was not robust enough to enable the fabrication of different dimensions to fit different patients. In addition, uniform tubes could not be easily utilized for holding vessels of different sizes next to each other during the anastomotic procedures. To address this challenge, we utilized 3D printers to fabricate sugar-based stents with desired dimensions and structures. The fabrication process and the utilization of the 3D-printed sugar-based stents are demonstrated in **Figure 1**a. The sugar-based materials were dissolved in water and placed in an oven under constant stirring until the majority of water (≈95% w/w) was evaporated. The molten sugar was then used as an ink to 3D-print tubular sugar-based stents. The fabricated sugar-based stents become sticky at the interface of moist surfaces. Once the vessels are placed over the stent, it holds them together and the surgeon can perform the anastomosis (Figure 1b). Once the blood flow is restored they will dissolve quickly without leaving a trace. A library of cylindrical sugar-based stents with different diameters fabricated by 3D printing is shown in Figure 1c.

Previously fabricated sugar-based stents contained mainly sucrose and glucose, which are biocompatible and possess high water solubility. However, the combination of glucose and sucrose forms a brittle sugar glass and can break into pieces upon exposure to mechanical loads, which is not suitable for use as vascular stents. To solve this problem, plasticizers should be added to the composition and we selected to use dextran, which has been approved for various food and medical uses by the United States Food and Drug Administration. The

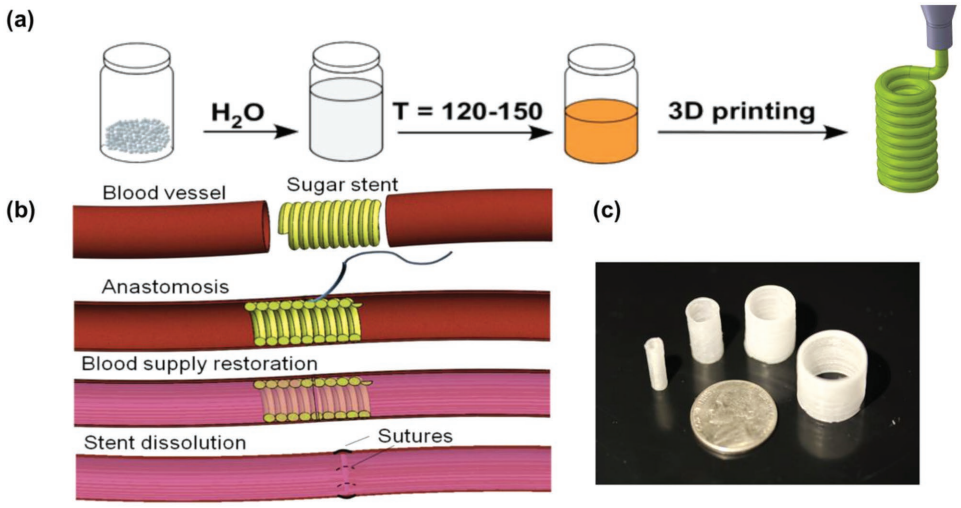

Figure 1. The fabrication and the utilization of sugar-based stents for vascular anastomosis. a) The process of preparation of sugar glass and its 3D printing into tubular stents. The mixture of sucrose, glucose, and dextran with water, after evaporating the majority of water in high temperatures (120–150 °C) were ready to 3D print. b) Schematic demonstration the utilization of 3D-printed sugar-based stents in surgical anastomosis. The sugar stent held the two vessels during suturing and was dissolved completely after blood supply restoration. c) Cylindrical sugar-based stents with various dimensions fabricated by 3D printing.

addition of dextran significantly improved the ductility of the formed sugar glass. It is noteworthy that the understanding of the chemical interactions between various compounds could be beneficial if further modifications is needed, especially if the sugar-based composition does not offer desirable properties.

The designed stent only holds the tissue in place for a few minutes and then dissolves in blood flow. However, surgeons can use surgical glues to adhere the tissue together during the anastomosis process. The effect of glucose concentration on the adhesion properties was studied through a standard lap shear test. For this reason, pig femoral arteries were obtained and cut into pieces of 1 cm × 2 cm and were glued on a glass slide. On another glass slide, the molten sugar was added and then the two slides were gently pressed together. The slides were fixed on grips of a mechanical tester and a tangential force was applied. The results showed an improvement in the adhesion strength by increasing glucose concentration ($p < 0.001$; **Figure 2**a).

One of the key parameters in the design and the use of stents is their interaction with blood and potential thrombogenicity. We tested the thrombogenicity of sucrose and glucose, and the results showed a reduction in the clotting time by an increase of glucose content, while sucrose prevented blood clot (Figure S1, Supporting Information). However, since glucose was important in adhesion strength to the vessel surface, optimizing the amount of sucrose and glucose in final composition to avoid thrombosis was important. The chance of clot formation in the presence of dynamic flow of blood could not be ruled out, especially in microvessels where the insertion of stents results in significant changes in hemodynamic. To avoid clotting effect of the engineered stent, we added sodium citrate, which is a calcium chelator and is currently used to prevent blood clot in clinic. Although the multicomponent nature of the sugar-based composition allows several methods for optimizing the properties of the stents, we only focused on the effect of ratio of components rather than their molecular weight. We varied the weight fractions of glucose (from 0 to 50% w/w), sucrose (from 0 to 50%w/w), dextran (from 0 to 20% w/w), and sodium citrate (from 0 to 5% w/w). The qualitative analysis showed that the composition of 11% (w/w) glucose, 69% (w/w) sucrose, 17% (w/w) dextran (86 kDa), and 3% (w/w) sodium citrate offered suitable mechanical, adhesion, ductility, and blood clotting properties to be used for forming stents. As can be seen in Figure 2b,c, the stents made from the modified sugar-based composition showed low thrombogenecity upon their use in blood vessels. It should be noted that the color of the sugar-based composition was dark brown and it should not be misidentified as clots that are formed around them.

We also measured the rheological properties of the selected material system to present how its time-dependent (energy absorbing) properties varied over a temperature range of 20 to 100 °C (Figure 2d). The viscous modulus, which indicates the capacity of material to dissipate mechanical energy, was found to be higher than the elastic modulus under shear loading. This could be interesting as the stent in situ would be subjected to dynamic loading by the blood vessels. At body temperature, the viscous and elastic moduli were in the range of 0.7–3.0 MPa. The elastic modulus and dynamic viscosity reduced logarithmically when the temperature rose up to 100 °C. This property of the material system was used to select an optimum temperature range for 3D printing of the construct. When the material is heated up in the nozzle, its viscosity (and elasticity) reduces to facilitate its flow through the nozzle. In our preliminary experiments, we found that a temperature range of 85–90 °C, which corresponded to a viscosity range of 50–70 Pa s, would be ideal for 3D printing with a nozzle gauge number of 18G or 20G.

We compared the mechanical properties of stents fabricated using the above composition with the compositions used in

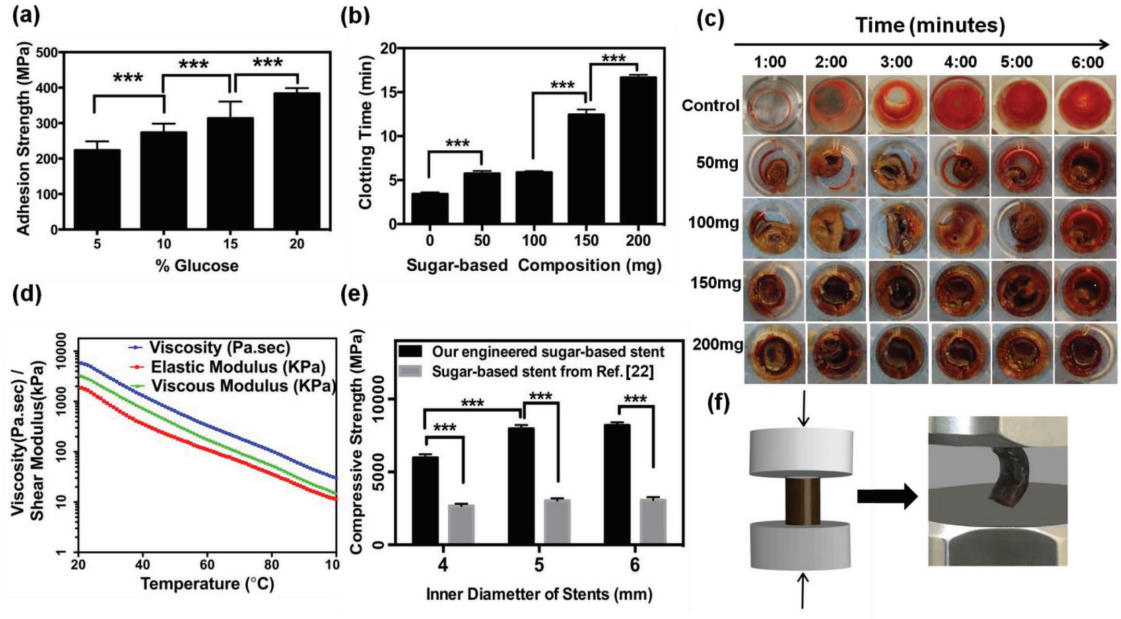

Figure 2. Evaluation of mechanical properties, adhesion strength, blood clotting time, and rheological properties of sugar-based composition. a) The effect of glucose concentration on the adhesion strength of sugar-based composition to atrial wall ($n = 3$). The glucose concentration in sugar composition had a direct relationship with adhesion strength of stents (***: $p < 0.001$). b,c) The clotting time assay of the sugar-based composition (11% (w/w) glucose, 69% (w/w) sucrose, 17% (w/w) dextran, and 3% (w/w) sodium citrate) shows that the optimized composition had low thrombogenecity ($n = 3$). d) Rheological characterization of the developed sugar-based stents. e) Comparative evaluation of the axial compressive strength of our engineered sugar-based stents ($n = 3$) and the stents made by the composition of ref. [22] with different diameters ($n = 3$) shows significantly higher mechanical properties of our sugar-based stents. f) The schematic illustration of sugar-based stents under compressive loads indicates the ductility of the constructs.

ref. [22] (29% (w/w) glucose, 60% (w/w) sucrose, and 11% (w/w) dextran; Figure 2e). As can be seen, by adding dextran into the sugar compound, the compression strength of stents improved significantly ($p < 0.001$). None of the samples fabricated using the proposed composition broke during the mechanical tests and they only were deformed. Figure 2f shows the schematic of the compressive mechanical test on sugar-based stents. The role of the stent is only to keep the arteries in place during the surgical procedure and then the stent dissolves rapidly. Therefore, the stent should only be stiff enough not to bend and deform during the anastomosis. The elastic modulus of our engineered sugar-based stent was 16 ± 2.3 MPa which is significantly higher than the values for arteries (1.54 ± 0.33 MPa) and veins (3.11 ± 0.65 MPa) reported by other researchers.[23]

To mimic the operation of the engineered stent and monitor its degradation rate, the stents were placed in transparent tubes, which were perfused by phosphate-buffered saline (PBS) at a rate of 20 mL min^{-1} (the flow rate comparable to small arteries; **Figure 3**a). At different time points, flow was stopped and the samples were removed and weighed, and the ratio of the dissolved mass was calculated. The results showed a gradual dissolution of the stent over time. We performed the experiments for tubes with an inner diameter of 3 mm and a variable outer diameter (Figure 3b). The results showed that the samples were dissolved between 4 and 6 min. During the perfusion time, the stents were gradually dissolved, while remained to the tube wall. The collected liquid was filtered to find broken pieces larger than 2 mm that were carried by the flow. During the experiments no indication of large pieces was observed. Although there might be some differences in flow pattern and consequently in the dynamic dissolution of sugar stents in Newtonian and non-Newtonian solutions, the differences will not be fundamentally different. To get close enough to in vivo conditions, we used the flow rate similar to blood flow and aqueous solution with temperature of 37 °C.

The total mass of a typical stent was around 600 mg and after dissolution of one sugar stent in whole blood volume, the variation in blood sugar level is negligible. However, during the dissolution time the local concentration of sugar could elevate for a few minutes. In addition, to ensure that no toxic compound is formed during the sugar-based material development, the sugar-based composition was dissolved in culture media at different concentrations and was used to treat culture of human umbilical vein endothelial cells (HUVECs). After 2 h, metabolic activity of the cells was measured using the PrestoBlue assay (**Figure 4**a). Results of the metabolic activity showed a high viability of endothelial cells after exposure to different concentrations of sugar for more than 2 h. As can be seen, the tested concentrations of sugar did not negatively impact cellular metabolic activity. After 24 h circulation of culture media containing 16% (w/v) sugar, live/dead assay and metabolic activity of cells showed no negative effect of high concentration of sugar on endothelial cells (Figure S2, Supporting Information).

In the next step, the effect of sugar-based stents on HUVECs was tested under dynamic culture. For this reason, a closed-loop fluidic circuit was developed in which HUVECs were cultured on a glass slide placed at the bottom of a bioreactor. Cells were exposed to flow-induced shear stress, which was mimicking their environment in the human body. Sugar-based

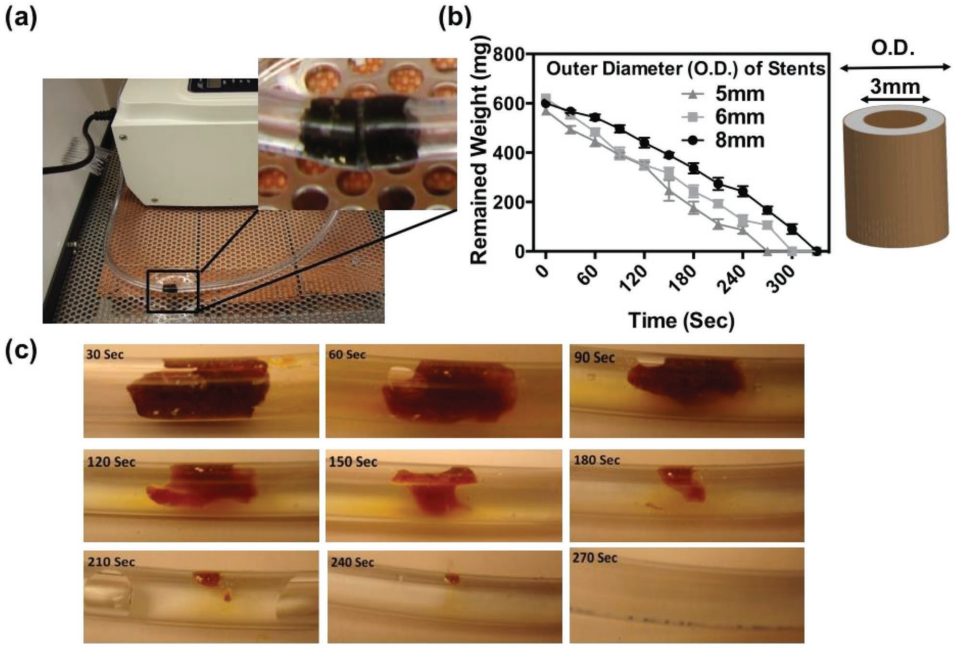

Figure 3. Assessment of the rate of sugar-based stent dissolution. a) The fluidic setup used for assessment of the dissolution of sugar-based stents and their dissolution pattern. b) The remaining weight of the engineered stents with an inner diameter of 3 mm and different outer diameter during PBS circulating ($n = 3$). The samples were gradually dissolved between 4 and 6 min and no large broken pieces were observed in the collected solution. c) Time-lapse images showing the gradual dissolution of the sugar stents and their adhesion to the tube wall during the stent dissolution.

stent was dissolved in 100 mL of culture media and poured in the reservoir to circulate through the system (Figure 4b). After 2 h circulation of the culture media containing sugar, cellular viability was visualized by the live/dead assay. In addition, to better understand the effect of each component of the sugar on HUVECs, similarly sized stents were fabricated from pure glucose and sucrose, were dissolved in 100 mL of culture media, and were perfused in separate bioreactors. The results showed that cells were alive, maintained their normal shape, and remained adherent to the glass slide (Figure 4c).

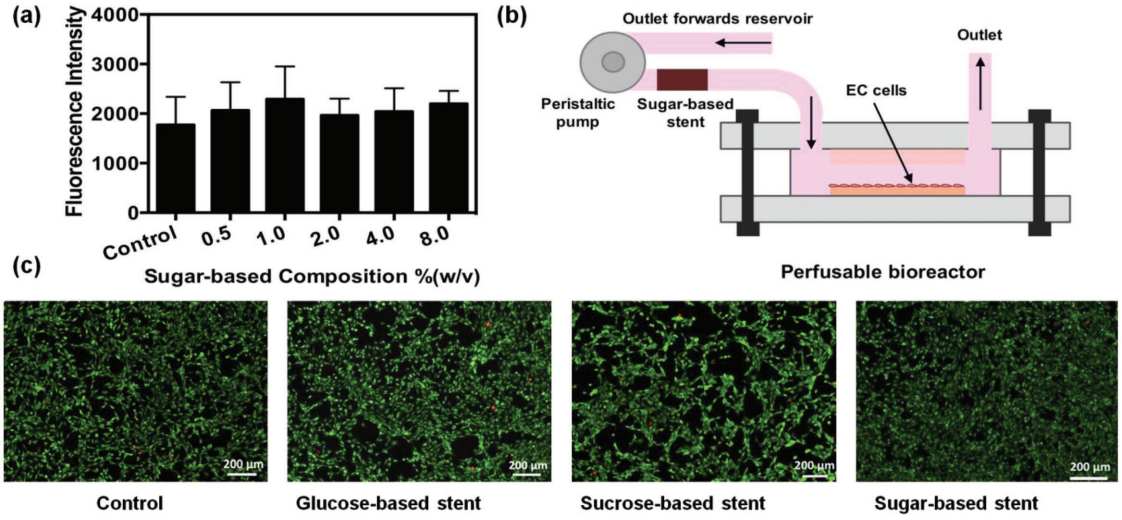

Figure 4. The biocompatibility assessment of sugar-based stent and its components on endothelial cells. a) Viability ratio of endothelial cells estimated by measuring their metabolic activity in static condition. Different concentrations of sugar were dissolved and placed over the cells ($n = 3$). Results were analyzed using PrestoBlue kit. The results showed high cellular viability after 2 h of culture media circulation. b) Schematic illustration of the custom-built bioreactor with a close-loop fluidic circuit. Endothelial cells were cultured on a glass slide and were placed inside the bioreactor. c) Fluorescence images of the live/dead assay performed on endothelial cells cultured within the bioreactor. Glucose-, sucrose-, and sugar-based stents were dissolved in culture media separately and put inside respected reservoir of microfluidic system. After 2 h of the dynamic experiment, the bioreactor was disassembled and endothelial cells were analyzed using live/dead assay kit. Live cells are presented as green and dead cells are shown in red color.

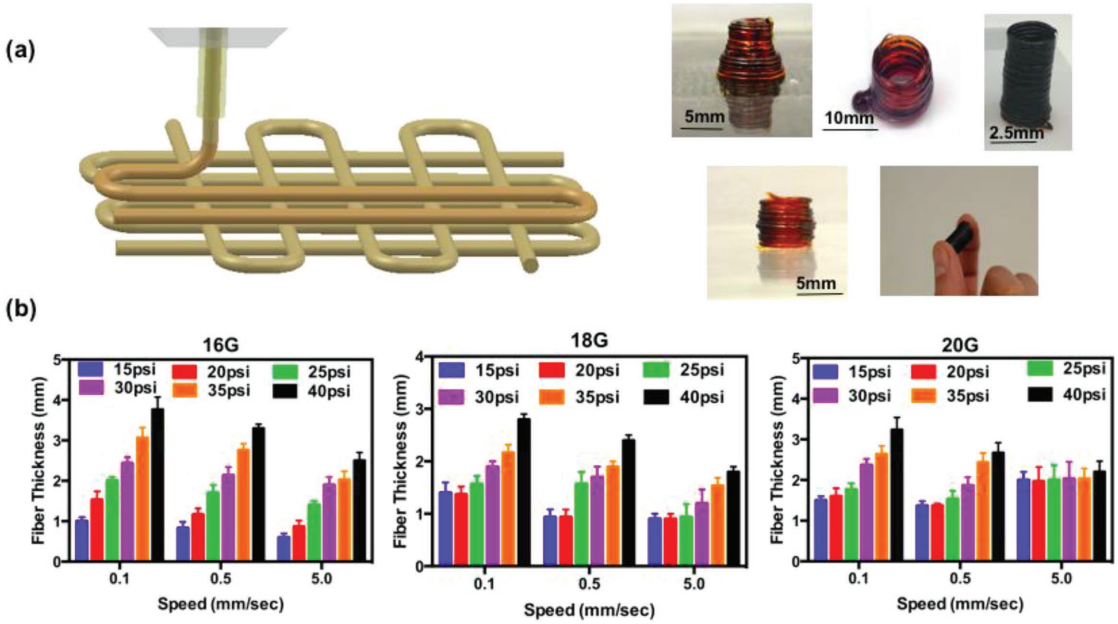

Figure 5. Assessment of the printability of the optimized sugar composition. a) Schematic of the 3D printing process and 3D-printed sugar stents. b) Effects of speed and nozzle diameter on the printing resolution: fiber thickness versus three nozzle speeds (low: 0.1 mm s^{-1}; medium: 0.5 mm s^{-1}; high: 5 mm s^{-1}) and pneumatic pressure (15–40 psi). Experiments were conducted three times for each condition.

The temperature of the solutions and materials in this study was kept less than 110° C for dissolving sucrose, glucose, and dextran in water, as well as remained water evaporation to avoid the potential formation of by-products such as furfural and heterocyclic, which usually are formed above 150 °C.[24] Regardless, our in vitro experiments confirmed the lack of toxicity in the formed sugar-based composition.

To assess the printability of the selected material system, we systematically investigated the influence of key 3D printing parameters on the generation of a continuous paste (**Figure 5**a). These key parameters included gauge number (nozzle diameter), nozzle speed, and pneumatic air pressure while the performance of 3D printing can be reported by the thickness of deposited straight line, or fiber. The air pressure dictated the pressure behind the nozzle while the material had a viscosity of 50–100 Pa s. We then measured the thickness of printed fibers, as the printing resolution, for various parameters as shown in Figure 5b. The results showed that by changing the nozzle diameter (from 16 to 20G where higher gauge number led to clogging issues) and the nozzle movement speed (from 0.1 to 5 mm s^{-1}), the thickness of the deposited fibers could be tuned in the range of 0.9 to 4 mm. We could also print tubular stents with different sizes and different shapes. In particular, connectors with different end sizes were printed that facilitate the anastomosis of nonequal sized vessels.

3D printing as a rapid fabrication technology provided a better control over the geometry of the fabricated constructs compared with conventional molding techniques. The viscosity of materials is a key factor in extrusion-based 3D printing. The temperature-dependent viscosity of our engineering materials allowed us to 3D print the sugar easily. The 3D printing technique offers the opportunity for rapid production of predefined, generally nonequal, anastomosis constructs in surgical rooms. Further technical advancement of 3D printing platforms, when interfaced with imaging modalities, may allow the fabrication of patient specific stents during the operation.

To assess the utility of the 3D-printed stents in facilitation of anastomosis, we performed two sets of experiments ex vivo. Pig femoral artery was explanted and cut into pieces and sugar-based tube connectors with around 5 mm outer and 4 mm inner diameters were used to connect the pieces of tissue and suturing was performed by a surgeon. Our experiments showed that through the use of the stent, the suturing time was reduced from approximately 15 min to less than 5 min. During the first set of experiments, the stent was inserted to hold the vessels and the suture was applied to seal the openings. We did not observe the slippage of the stent during the suturing process and the stents remained intact during the process. Upon the completion of the anastomosis, the vessels were perfused with aqueous solutions containing food dye with the rate of 35 mL min^{-1} and no leakage was observed. After a few minutes, the flow was stopped and the vessels were cut. The stent was completely dissolved and we did not observe any large pieces of sugar within the vessel or in the collected solution (**Figure 6**a).

During the second set of experiment, a thicker-walled stent with 5 ± 1 mm of outer diameter and 3 ± 1 mm of inner diameter was used and after the first couple of sutures, aqueous solution was flowed through the vessels. No leakage was observed during the suturing process despite the continuation of the liquid perfusion. Immediately after suturing, the flow was stopped and the sutured were cut and the sugar stent was inspected. We noticed that the stent had become thinner while no pieces were broken (Figure 6b). The traditional surgical

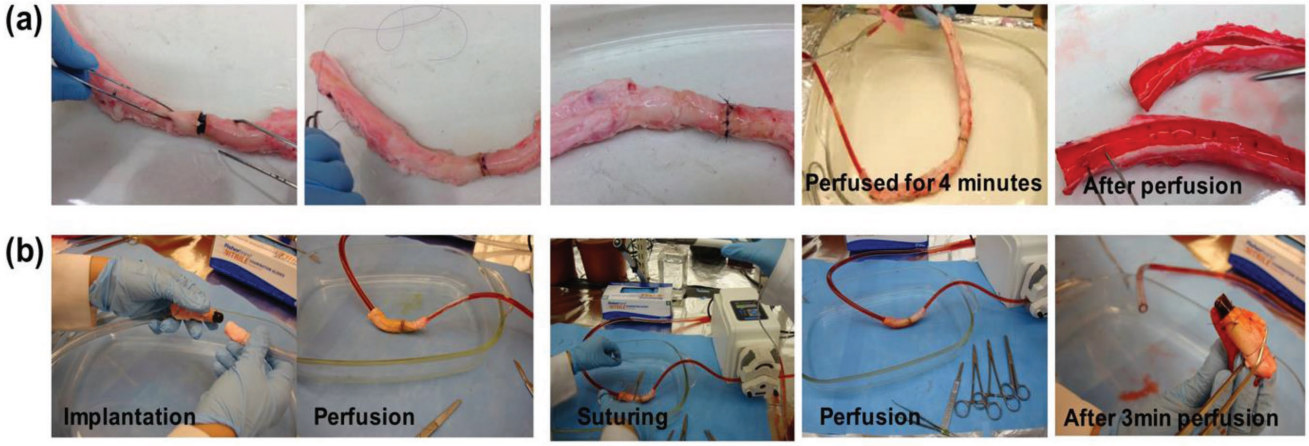

Figure 6. Ex vivo use of the sugar-based stents in suture-based anastomosis. a) A rapidly dissolvable stent was applied and pig arteries were connected by suturing. After that the vessels were perfused by aqueous solutions containing food dye at the rate of 35 mL min^{-1} and the stent was completely dissolved. No blood leakage was observed. b) A stent with longer dissolution time was used. The stent held the vessels together and perfusion was started. Suturing was continued without interruption of perfusion and no leakage was observed during and after anastomosis.

technique for microvascular anastomosis involves stopping the blood flow using a clamp, holding the vessel sides next to each other, and connecting them by using microvascular sutures under microscopic magnification.[25] Disadvantages of this method include the increased time needed for suturing, stopped sending the nutrition and oxygen to the tissues during suturing, and damaged live tissues during suturing. By using sugar-based stents during suturing, there is no need for stopping the blood flow, which can potentially improve the outcome of the surgical procedure.

Overall, the proposed dissolvable stents facilitate vascular anastomosis. It is hemocompatible and does not induce thrombosis; its adhesion to the wet tissue eliminate combined by its rigidity, facilitates the suture-based microanastomosis.

3. Conclusions

Nonbrittle and anticlotting sugar-based composition was developed and used as the ink in commercially available 3D printers to create stent-like structures that could facilitate surgical anastomosis. The stents were completely dissolvable and their rate of dissolution and mechanical properties were tunable by changing the material composition. The sutures could hold the vessels in place during the suturing process and prevent the possibility of back-suturing during microsurgeries. The stents prevented thrombosis and blood leakage during the procedure. The 3D printing process that enabled us to fabricate constructs with desired shape and dimension was fast and a stent could be formed in less than few minutes. Thus, this technology can be used for printing the stents with correct dimension during the operation to improve the surgical outcome. In addition, the closed structure of the stents can prevent the leakage of surgical glues into vessels and in future can facilitate the suture-free anastomosis through combination with surgical glues. In future, animal studies should be conducted to ensure the effectiveness of the developed stents in facilitating surgical anastomosis.

4. Experimental Section

Materials: All chemical were purchased from Sigma-Aldrich while the cell culture medium and regents were obtained from Invitrogen unless mentioned otherwise.

Preparation of Sugar Glass and Stents: Two sets of sugar compounds were formed, one by mixing of 9.7 g glucose, 61 g sucrose, 15 g dextran, and 3 g sodium citrate. The incorporation of dextran improved the flexibility and incorporation of sodium citrate increased blood clotting time of the sugar-based composition. Another set of sugar compound was made from ref. [22] by mixing of 25 g glucose, 53 g sucrose, and 10 g dextran. The mixture was dissolved in 50 mL of distilled water and the solution was stirred for 3 h at 130 °C to evaporate most of the water and form a liquid glass. The liquid glass was poured into glass syringe and was used in an extrusion-based printer (Allevi, Inc, Philadelphia, PA) to 3D print the engineered sugar glass. The printer involved a custom-built reservoir connected to a high-pressure air source. The reservoir was heated up to 120 °C to lower the viscosity of sugar. Different shapes of sugar structures were prepared by the 3D printer under nitrogen pressure with pneumatic control through a 16-, 18-, and 20-gauge steel nozzle. Sugar tubes were also formed using molding in which molten sugar glass was added into PDMS molds and the samples were cured at 170 °C for about 2 h.

Mechanical Characterization of the Material and Fabricated Stents: A standard lap shear stress was performed to assess the adhesion properties of the engineered sugar to native tissues. For this reason, a pig femoral artery was purchased and was cut into 1 cm × 2 cm pieces which were glued onto glass slide. The sugar glass was poured and cured onto glass slides to cover a similar area. A sugar coated slide was placed on top of the tissue glued to the glass slide. The two slides were loaded into the grips of an Instron 5542 mechanical tester (Norwood, MA, USA). The samples were stretched and the adhesion strength was recorded.

The compressive mechanical properties of sugar-based stents were also determined. For this reason, cylindrical sugar-based stents were generated and were placed between the grips of the Instron mechanical tester and were compressed in axial direction.

Rheological Characterization of Sugar: The rheological properties of the sugar-based composition were measured using a controlled stress AR-G2 rheometer (TA Instruments, New Castle, DE) with a 40 mm diameter, parallel-plate geometry. The shear storage modulus (G'), the loss modulus (G''), and dynamic viscosity (/eta) were measured at a frequency of 1 Hz and an oscillatory strain of 0.05 (i.e., 5%). Temperature sweeps were performed using a Peltier plate (to heat up the bottom surface) over the range of 20 to 120 °C. Samples were equilibrated for

1 min before testing and for 30 s at each subsequent temperature to ensure thermal homogeneity throughout the sample.

Clotting Time Assay: Approximately 50 mg of glucose, sucrose, or the sugar-based composition was placed at the bottom of each well in 48 well flat-bottom plate. Mixture of 90% (v/v) citrated blood and 0.1 M calcium chloride was vortexed for 15 s and 100 µL of blood solution was deposited into sequential wells on a 48-well plate. Saline solution with concentration of 9 g L^{-1} was used to wash each well at selected time points to halt clotting. The liquid was immediately aspirated and washes repeated until the solution was clear, indicating removal of all soluble blood components. Final clotting time was marked in the well that formed a uniform clot, with no change in clot size in subsequent wells.

Assessment of the Dissolution Rate of Sugar Tubes: To mimic the operation of the engineered stent and monitor its degradation rate, the stents were placed in transparent acrylic tubes with the thickness of 2 mm, which were perfused by PBS with a rate of 20 mL min^{-1} (the flow rate comparable to small arteries). At different time points flow was stopped and the samples were removed and weighed and the ratio of the dissolved mass was calculated.

Biocompatibility Assessment of the Engineered Sugar-Based Stent: HUVECs were cultured in endothelial culture media obtained from Lonza and were used up to passage 9. Biocompatibility of the engineered sugar-based stent was analyzed in static and dynamic conditions. In static tests, HUVECs were cultured in well plates. Sugar stents were dissolved in culture media and put over the endothelial cells. After 2 h, media containing sugar was aspired and the viability of the cells was analyzed using new media containing PrestoBlue reagent (Thermo Fisher) with the ratio of 1:10. Cells were incubated for about half an hour at 37 °C. Thereafter, the media over the cells were collected and read by the plate reader.

Bioreactor for dynamic tests consisted of two parts, fluidic and holder of the glass slide. All bioreactor parts were made of polydimethylsiloxane (PDMS, Sylgard 184 Elastomer Kit, Dow Corning, weight ratio monomer to crosslinking agent 10:1). Uncured PDMS was poured over poly(methyl methacrylate) (PMMA) molds and put under desiccator until all of the bubbles inside the solution would be disappear. Then, the molds containing PDMS put inside +80 °C oven overnight till the PDMS would be totally cured. Slide glasses were cut into appropriate sizes to fit in the holder part of the bioreactor. All PDMS parts, tubes and slide glasses were put inside the autoclave machine in order to be sterile. HUVECs were cultured over the glass slides and put inside the incubator until a homogeneous monolayer of cells was formed. Next, glass slide was put inside the bioreactor and all parts were fixed using sterile screws. The bioreactor was connected to the reservoir using tubes which were appropriate for the peristaltic pump. Sugar, glucose, and sucrose stents were dissolved in 100 mL of culture media and added to the reservoir. The whole fluidic system was run for 2 h. After 2 h, the bioreactors were disassembled and glass slides containing HUVECs were removed and treated with LIVE/DEAD Viability/Cytotoxicity Kit (Theromo Fisher) for 15 min at 37 °C. At final stage, stained cells were analyzed using fluorescent microscope where live cells could be detected with green and dead cells could be identified with red labels.

Statistical Analysis: Each experiment was repeated three times and all data were presented by means ± standard deviation. Data were analyzed using one- and two-ways ANOVA and significant differences were presented as $*p < 0.05$, $**p < 0.01$, and $***p < 0.001$.

Supporting Information

Supporting Information is available from the Wiley Online Library or from the author.

Acknowledgements

R.S. is a founder of Allevi INC, which is a manufacturer of Allevi 3D printers. This research was partially supported by the National Institutes of Health (HL092836, DE019024, EB012597, AR057837, DE021468, HL099073, AR073822, GM126831). A.T. acknowledges financial support from the University of Nebraska-Lincoln and Nebraska Tobacco Settlement Biomedical Research Enhancement Funds.

Conflict of Interest

R.S. is a founder of Allevi INC, which is a manufacturer of Allevi 3D printers.

Keywords

3D printing, dissolvable stents, personalized surgical tools, sugar-based materials, vascular anastomosis

Received: June 18, 2018
Revised: September 10, 2018
Published online: October 30, 2018

[1] a) C. Zeebregts, R. Heijmen, J. Van den Dungen, R. Van Schilfgaarde, *Br. J. Surg.* **2003**, *90*, 261; b) I. Ducic, B. J. Brown, S. S. Rao, *Microsurgery* **2011**, *31*, 360; c) T. Zhang, D. Dyalram-Silverberg, T. Bui, J. Caccamese, J. Lubek, *Int. J. Oral Surg.* **2012**, *41*, 751; d) V. A. Byvaltsev, S. K. Akshulakov, R. A. Polkin, S. V. Ochkal, I. A. Stepanov, Y. T. Makhambetov, T. T. Kerimbayev, M. Staren, E. Belykh, M. C. Preul, *Minimally Invasive Surg.* **2018**, *2018*, 6130286.

[2] a) R. K. Khouri, B. C. Cooley, A. R. Kunselman, J. R. Landis, P. Yeramian, D. Ingram, N. Natarajan, C. O. Benes, C. Wallemark, *Plast. Reconstr. Surg.* **1998**, *102*, 711; b) C. Lebowitz, J. L. Matzon, *Hand Clin.* **2018**, *34*, 85.

[3] a) L.-E. Chen, A. V. Seaber, J. R. Urbaniak, *J. Reconstr. Microsurg.* **1993**, *9*, 183; b) J. M. Serletti, M. A. Deuber, P. M. Guidera, G. Reading, H. R. Herrera, V. F. Reale, J. R. Wray, V. Y. Bakamjian, *Plast. Reconstr. Surg.* **1995**, *95*, 270.

[4] G. Hallock, D. Rice, *J. Hand Microsurg.* **2009**, *01*, 3.

[5] J. W. Frederick, L. Sweeny, W. R. Carroll, E. L. Rosenthal, *Otolaryngol.–Head and Neck Surg.* **2013**, *149*, 67.

[6] M. Just, C. Chalopin, M. Unger, D. Halama, T. Neumuth, A. Dietz, M. Fischer, *Eur. Arch. Oto-Rhino-Laryngol.* **2016**, *273*, 2659.

[7] W. Schiller, H. Rudorf, C. B. Welzel, M. J. Kiderlen, C. Probst, O. Dewald, A. Welz, *J. Thorac. Cardiovasc. Surg.* **2007**, *134*, 1513.

[8] A. Leppäniemi, D. Wherry, E. Pikoulis, H. Hufnagel, C. Waasdorp, N. Fishback, N. Rich, *J. Vascul. Surg.* **1997**, *26*, 24.

[9] G. A. Giessler, G. T. Fischborn, A. B. Schmidt, *J. Plast. Reconstr. Aesthetic Surg.* **2012**, *65*, 100.

[10] a) C. Isles, S. Robertson, D. Hill, *QJM* **1999**, *92*, 159; b) G. D. Lang, C. Fritz, T. Bhat, K. K. Das, F. M. Murad, D. S. Early, S. A. Edmundowicz, V. M. Kushnir, D. K. Mullady, *Gastrointest. Endoscopy* **2018**, *87*, 150.

[11] a) R. V. Marrey, R. Burgermeister, R. B. Grishaber, R. Ritchie, *Biomaterials* **2006**, *27*, 1988; b) R. J. van Bommel, M. E. Lemmert, N. M. van Mieghem, R. J. van Geuns, R. T. van Domburg, J. Daemen, *Catheterization Cardiovasc. Interventions* **2018**, *91*, E21; c) J. Univers, C. Long, S. A. Tonks, M. B. Freeman, *J. Vascul. Surg.* **2018**, *67*, 615.

[12] P. K. Bowen, R. J. GuilloryII, E. R. Shearier, J.-M. Seitz, J. Drelich, M. Bocks, F. Zhao, J. Goldman, *Mater. Sci. Eng., C* **2015**, *56*, 467.

[13] X. Wang, Y. Yan, R. Zhang, Y. Fan, F. Cui, Q. Feng, X. Liang, *J. Bioact. Compat. Polym.* **2004**, *19*, 409.

[14] M. Shechter, C. N. B. Merz, M. J. Paul-Labrador, S. Kaul, *J. Am. Coll. Cardiol.* **2000**, *35*, 300.

[15] X. H. Wang, X. Liang, Z. Xiong, Y. N. Yan, R. Zhang, F. Lin, R. D. Wu, Q. P. Lu, Y. W. Fang, presented at *Key Eng. Mater*. **2005**, pp. 575–578.
[16] A. Power, N. Duncan, S. K. Singh, W. Brown, E. Dalby, C. Edwards, K. Lynch, V. Prout, T. Cairns, M. Griffith, *Am. J. Kidney Dis.* **2009**, *53*, 1034.
[17] G. Lee, G. M. Arepally, *J. Clin. Apheresis* **2012**, *27*, 117.
[18] D. M. Adcock, D. C. Kressin, R. A. Marlar, *Am. J. Clin. Pathol.* **1997**, *107*, 105.
[19] a) B. Zhang, Y. Luo, L. Ma, L. Gao, Y. Li, Q. Xue, H. Yang, Z. Cui, *Bio-Design Manuf.* **2018**, *1*, 211; b) N. Faramarzi, I. K. Yazdi, M. Nabavinia, A. Gemma, A. Fanelli, A. Caizzone, L. M. Ptaszek, I. Sinha, A. Khademhosseini, J. N. Ruskin, A. Tamayol, *Adv. Healthcare Mater.* **2018**, *7*, 1701347.
[20] M. Mohammadi, S. A. Mousavi Shaegh, M. Alibolandi, M. H. Ebrahimzadeh, A. Tamayol, M. R. Jaafari, M. Ramezani, *J. Controlled Release* **2018**, *274*, 35.
[21] N. Annabi, A. Tamayol, J. A. Uquillas, M. Akbari, L. E. Bertassoni, C. Cha, G. Camci-Unal, M. R. Dokmeci, N. A. Peppas, A. Khademhosseini, *Adv. Mater.* **2014**, *26*, 85.
[22] J. S. Miller, K. R. Stevens, M. T. Yang, B. M. Baker, D.-H. T. Nguyen, D. M. Cohen, E. Toro, A. A. Chen, P. A. Galie, X. Yu, R. Chaturvedi, S. N. Bhatia, C. S. Chen, *Nat. Mater.* **2012**, *11*, 768.
[23] F. Pukacki, T. Jankowski, M. Gabriel, G. Oszkinis, Z. Krasinski, S. Zapalski, *Eur. J. Vasc. Endovasc. Surg.* **2000**, *20*, 21.
[24] a) M. S. Bergdoll, E. Holmes, *J. Food Sci.* **1951**, *16*, 50; b) Y. Houminer, S. Patai, *Isr. J. Chem.* **1969**, *7*, 513.
[25] P. M. Werker, M. Kon, *Ann. Thorac. Surg.* **1997**, *63*, S122.